Pickup Manipulator Design and Its Kinematics Simulation

Zhongdang Zhang[1, 2], Zhaoqiang Zhang[1, 2], Shitai Ma[1, 2] and Haibo Zhou[1, 2, *]

[1]Tianjin University of Technology Tianjin Key Laboratory for Advanced Mechatronic System Design and Intelligent Control, Tianjin 300384, China
[2]National Demonstration Center for Experimental Mechanical and electrical Engineering Education (Tianjin University of Technology), Tianjin 300384, China

*Corresponding author e-mail: haibo_zhou@163.com.

Abstract. In order to improve the flexibility of the pickup manipulator and solve the problem of picking up small sports balls in training ground such as golfing, tennis, and table tennis, a 5-DOF pickup manipulator structure is designed. According to the pickup task requirements of the manipulator, through theoretical calculations, the 86HS series stepping motor is selected as the driving motors of the front end joints. Based on this, the stepping motor control system is designed to realize the closed-loop control of the manipulator. Then the manipulator model is built using D-H method, the inverse kinematics solution is calculated, and the analysis of kinematic theory is conducted. Finally, the targeted pickup point is selected to carry out case simulation analysis of the manipulator, the motion law of the manipulator is verified to be reasonable and the task of picking up small sports balls is completed.

1. Introduction

Compared with the defects of traditional manual pickup operations, such as high labor intensity, high risk and low efficiency, the manipulator has flexible operation and can replace manpower to complete tasks such as picking up and grasping. It has wide application prospects, and has become a hot research topic at home and abroad [1, 2, 3]. In view of the problem of picking up small balls such as table tennis, tennis, and golf balls in the training ground, many scholars have done relevant research. As early as 1995, Pacheco L and Ribeiro et al. [4] began to develop physical prototypes for picking up golf balls. By 2012, Nino Pereira and Daniel Whitney [5, 6] jointly developed a clamped golf ball harvester that successfully achieved the functions of autonomous navigation, obstacle avoidance, and ball pickup. In recent years, the development of domestic pick-up robots has also begun. In 2013, Lv Tengfei and Lu Li invented [7] intelligent tennis pickup machine, which was composed of sports system, vision system and pickup part, completed the search and pickup of tennis. In 2016, Sun Shijun and He Xueliang [8] developed a tennis pick-up robot system based on visual capture to pick up tennis scattered on tennis courts by robotic arms mounted on mobile robot platforms.

However, the operating flexibility of the existing pickup mechanism is poor, the generality is not strong, and the operation is greatly influenced by the environment. In view of the deficiencies of the above research contents, taking the characteristics of multi-degree-of-freedom manipulator into full consideration, such as flexible operation and strong environmental adaptation, a 5-DOF pickup manipulator is designed to carry out pickup operation on small sports balls in the training ground. Through the theoretical calculation, the 86HS series stepping motor is selected as the driving motor for

the joints 1, 2 and 3, and the stepping motor system design is completed to achieve the closed-loop control. Based on the D-H method [9, 10], the kinematics model of the manipulator is established and the inverse kinematics solution is solved. The case simulation analysis of the manipulator is realized by means of programming in the MATLAB software, and finally the purpose of picking up small sports balls is achieved.

2. Structure design of the manipulator

Fig. 1 shows the overall structure of the manipulator, which is mainly composed of a base, joints, joint connecting rods and end clamping devices. It is used to imitate the human arm to complete the autonomous pickup tasks of small ball objects. The selection of the degree of freedom of the manipulator involves issues such as the degree of difficulty or ease of the calculation, movement flexibility and precision of control. With the increase in the degree of freedom, the flexibility and generality of the manipulator increase, but the structure is more complex, the calculation is more difficult, and the control accuracy is reduced. Therefore, choosing a reasonable number of degree of freedom is crucial to the manipulator's structural design. Referring to the human arm movement function, considering the task requirements of the manipulator and the factors affecting the degree of freedom, the articulated manipulator structure with 5-DOF is determined. In order to facilitate the control of the manipulator and improve the motion precision and drive efficiency, all joints are driven by the motor.

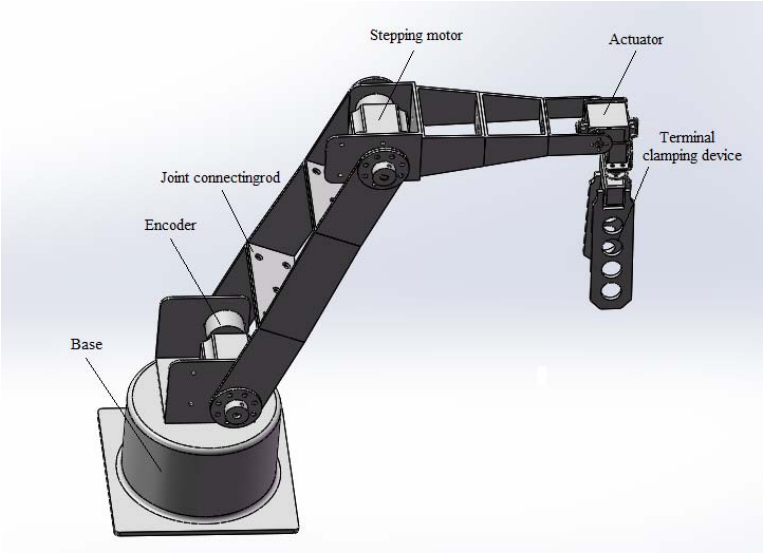

Figure 1. Schematic diagram of the manipulator

The base is fixed on the moving body and is used to support the motion of the manipulator. Joint 1, joint 2 and joint 3 are respectively composed of U-shaped support frame, the drive motor and HK50-D8G encoder. The motor is used to drive the joint connecting rod, and the encoder can monitor the motion state of the joint in real time to ensure the precision of the control. The joint 1 imitates the rotation of the human shoulder joint to achieve the manipulator's peripheral rotational movement and expands the small ball object's pick-up space. Joints 2 and 3 imitate the two joints of the human shoulder and elbow to realize the upper and lower pitch motion of the manipulator and adjust the distance of picking up balls. The MG996R rudder has lighter overall quality and less space, which is used for the drive of joints 4 and 5. They imitate human wrist movements to change the pose of the end effector in a small range so as to be easy to grab. The terminal clamping device is similar to two human fingers. By controlling the tensioning of the two finger joints, the target object is grasped and the pickup task is completed in the training ground.

3. Drive motor selection and control system

3.1. Drive motor selection

The driving motor of the manipulator is mainly divided into three types: servo motor, rudder and stepping motor. Because stepping motor has the characteristics of precise positioning, simple operation and stable performance, and the matching stepping driver has the advantages of optional mode, subdivision driving and torque smoothing at the low speed, the stepping motor is selected as the driving motor of the manipulator.

The quality of the joints 1, 2, 3, 4 and 5 is roughly obtained through SolidWorks software. They are respectively m_1=2.5kg, m_2=2.5kg, m_3=2.5kg, m_4=0.1kg and m_5=0.2kg. The lengths of joint connecting rods 1, 2 and 3 are respectively a_1=22mm, a_2=330mm, a_3=210mm, and the length of the terminal clamping device is l=90mm. According to the requirements of the pickup task of the manipulator, the pickup speed should be above 400PCS/h. When setting a single task, the process time of picking up and placing is divided equally, namely, t=4.5s, the rotation angle θ of various joints is limited to 150°, and the maximum angular velocity w_{max} is reached after 0.2s of acceleration, thus the angular acceleration α can be obtained:

$$\begin{cases} \theta_{max} = 0.4 * \omega_{max} / 2 + 4.1 * \omega_{max} \\ \alpha = \Delta\omega / \Delta t = \omega_{max} / \Delta t \end{cases} \tag{1}$$

Selecting the joints 1, 2 and 3 to analyze the motor torque. Since the moments of inertia of the joints around their Z-axis of gravity are respectively J_{G1}, J_{G2}, and J_{G3}, according to the parallel axis theorem, the moment of inertia of J_i at each joint is given by:

$$J_i = \sum_{j=i}^{n} J_{Gj} + \sum_{j=i}^{n} m_j l_j^2 \tag{2}$$

Because $J_{Gi} << m_i l_i^2$, the size of the J_{Gi} can be ignored, J_i can be formulated as:

$$J_i = \sum_{j=i}^{n} m_j l_j^2 \tag{3}$$

Taking the ultimate position of the manipulator to calculate the total torque M_i that the stepping motor should be able to reach under the load starting.

$$M_i = M_{Ji} + M_{Ti} \tag{4}$$

$$\begin{cases} M_{Ji} = J_i \alpha \\ M_{Ti} = \sum_{j=i}^{n} m_j g l_j \end{cases} \tag{5}$$

In the formula (4): M_{Ji} - motor starting inertia torque; M_{Ti} - accumulate load torque.

According to calculation results: M_1=1.0N·m, M_2=10.73N·m and M_3=0.85N·m. Taking into account the influence of external factors, the safety factor is set to 2. Thus, M_{1min}=2.62N·m, M_{2min}=22.02N·m, M_{3min}=1.72N·m. Under the condition that the reduction ratio is 5, the minimum torque of the stepping motor at the second joint should satisfy $M_{2motor}=M_{2min}/5$=4.4N·m.

When the stepping motor moves in the allowable range of the speed, the torque must be maintained to meet the requirement of the joint torque. Referring to the parameters of the 86HS series stepping

motor showed in Table 1, the 86HS35, 86HS45 and 86HS35 stepping motors are selected as the drive motors for the joints 1, 2 and 3, and the TB6600 stepping motor driver is configured.

Table 1. 86HS series stepping motor parameter table

Model	Phase	Step angle (°)	Holding torque (N·m)	Rated current (A)	Phase inductance (mH)	Phase resistance (Ohm)	Number of leads
86HS35	2	1.8	3.5	2.8	3.9	1.4	8
86HS45	2	1.8	4.5	4.0	3.5	0.8	8
86HS65	2	1.8	6.5	4.0	3.5	0.8	8
86HS85	2	1.8	8.5	4.2	6	0.9	8
86HS120	2	1.8	12	4.2	8	1.25	8

3.2. Design of motor control system

Stepping motor control system is mainly composed of STM32 control board, TB6600 stepping motor driver, 86HS series stepping motor and HK50-D8G encoder. The overall design is showed in Fig. 2.

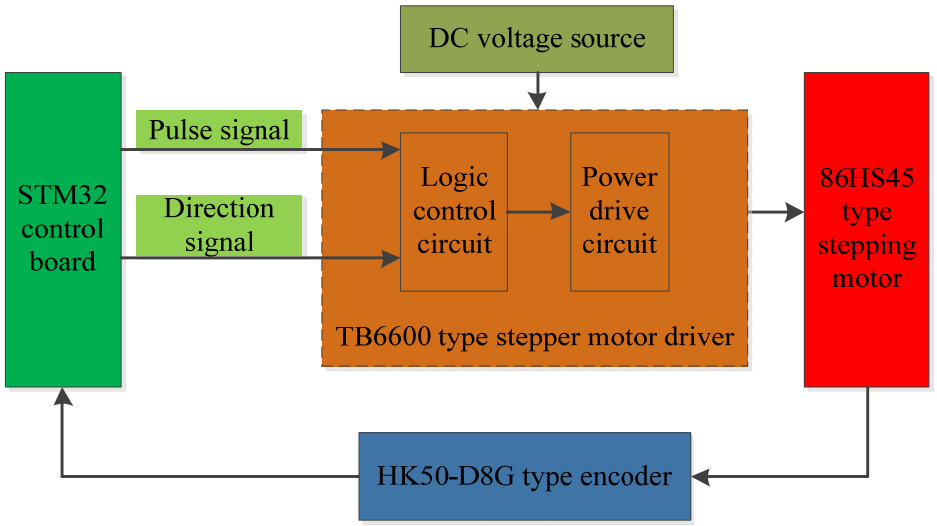

Figure 2. Stepping motor control system

The STM32 control board serves as a system controller for issuing pulse and steering signals. The pulse frequency determines the start-stop or speed of the stepping motor, and the steering signal determines the rotation direction of the stepping motor. The stepping motor driver is mainly composed of a logic control circuit and a power drive circuit, which accepts the controller signal and drives the stepping motor. According to the control signal, the logic control circuit generates a turn-on or turn-off signal of the excitation windings of each phase of the stepping motor with the preset motor energization mode. The power drive circuit amplifies the output signal power and drives the rotor to move. The stepping motor, as an actuator, converts the received electric pulse signal to the corresponding angular displacement to realize the rotation of each joint. Under non-overload conditions, the speed of stepping motor is proportional to the pulse frequency, and the motor speed and angular displacement can be controlled by controlling the pulse frequency. In order to improve the manipulator's movement accuracy, a HK50-D8G encoder is added to the joint. The monitored angular displacement signal is fed back to the STM32 control board in real time, the controller processes the feedback signal and issues corresponding instructions to achieve the closed-loop control.

4. Kinematic analysis and simulation

4.1. Kinematics Modeling

The pickup manipulator is made up of 5 rotating joints in series connection. According to the simplified model of manipulator showed in Fig. 3 (a), the linkage coordinate system showed in Fig. 3 (b) is established based on D-H method. The D-H parameter table showed in Table 2 is determined by the linkage coordinate system established in Fig. 3, where θ_i represents the linkage rotation angle, a_{i-1} represents the linkage length, α_{i-1} represents the linkage twist angle, and d_i represents the linkage offset distance.

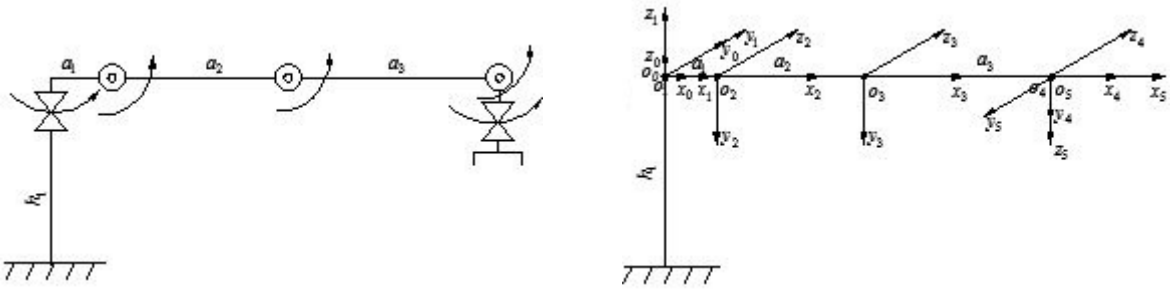

(a) Structural schematic diagram (b) Linkage coordinate system

Figure 3. Linkage coordinate system of the manipulator

Table 2. D-H parameter list of the manipulator

Linkage i	θ_i	α_{i-1}	a_{i-1}	d_i	Variable range
1	θ_1	0°	0	0	-45°~45°
2	θ_2	-90°	a_1	0	-135°~10°
3	θ_3	0°	a_2	0	-90°~90°
4	θ_4	0°	a_3	0	-240°~60°
5	θ_5	-90°	0	0	-45°~45°

According to the established linkage coordinate system and D-H parameter table, the homogeneous transfer matrix of the coordinate system {i} relative to the coordinate system {i-1} between adjacent connecting rods is obtained, as shown in formula (6). Based on this, the pose of the manipulator end coordinate system o_5 corresponding to the base coordinate system o_0 can be solved. As shown in formula (7), the kinematic model of the manipulator is established.

$$ {}^{i-1}_{i}T = \begin{bmatrix} c\theta_i & -s\theta_i & 0 & a_{i-1} \\ s\theta_i c\alpha_{i-1} & c\theta_i c\alpha_{i-1} & -s\alpha_{i-1} & -d_i s\alpha_{i-1} \\ s\theta_i s\alpha_{i-1} & c\theta_i s\alpha_{i-1} & c\alpha_{i-1} & d_i c\alpha_{i-1} \\ 0 & 0 & 0 & 1 \end{bmatrix} \tag{6} $$

$$ {}^{0}_{5}T = {}^{0}_{1}T(\theta_1){}^{1}_{2}T(\theta_2){}^{2}_{3}T(\theta_3){}^{3}_{4}T(\theta_4){}^{4}_{5}T(\theta_5) = \begin{bmatrix} n_x & o_x & a_x & p_x \\ n_y & o_y & a_y & p_y \\ n_z & o_z & a_z & p_z \\ 0 & 0 & 0 & 1 \end{bmatrix} \tag{7} $$

4.2. Inverse kinematics solution

The inverse kinematics of the manipulator is to calculate the joint angles through the pose of the end clamping device. According to the formula (7), through the known terminal pose matrix, the inverse kinematics is solved by the inverse transform method [11, 12]. The results are showed in formulas (8) ~ (12).

$$\theta_1 = a\tan2(p_y, p_x) \tag{8}$$

$$\theta_2 = a\tan2\frac{\pm\sqrt{1-A^2}}{A} \tag{9}$$

$$\theta_3 = a\tan2\frac{\pm\sqrt{4a_2^2a_3^2-\left[(c_1p_x+s_1p_y-a_1)^2+p_z^2-a_2^2-a_3^2\right]^2}}{(c_1p_x+s_1p_y-a_1)^2+p_z^2-a_2^2-a_3^2} \tag{10}$$

$$\theta_4 = a\tan2\frac{-c_1c_{23}a_x-s_1c_{23}a_y+s_{23}a_z}{\pm\sqrt{1-(c_1c_{23}a_x+s_1c_{23}a_y-s_{23}a_z)^2}} \tag{11}$$

$$\theta_5 = a\tan2\frac{s_1n_x-c_1n_y}{\pm\sqrt{1-s_1^2n_x^2-c_1^2n_y^2+2s_1c_1n_xn_y}} \tag{12}$$

Among them, $A=\dfrac{a_2c_1p_x-a_1a_3c_3-a_1a_2+a_2p_ys_1-a_3p_zs_3+a_3c_3p_ys_1+a_3c_1c_3p_x}{a_1^2-2a_1c_1p_x-2a_1p_ys_1+c_1^2p_x^2+2c_1p_xp_ys_1+p_y^2s_1^2+p_z^2}$

4.3. Kinematics simulation

With the MATLAB tool, the targeted pickup point is selected to carry out case simulation analysis of the manipulator. According to the inverse kinematic solution, the joint angles corresponding to point A are respectively (0°, -9.3°, 84.2°, -74.9°, 0°). Under continuously operating state, the manipulator is set to pick up balls at the speed of 400PCS/h, and each of the picking up and placing processes takes 4.5s. Then cubic polynomial interpolation method [13] is used to simulate the motion curve of the pickup process. The results are showed in Fig. 4.

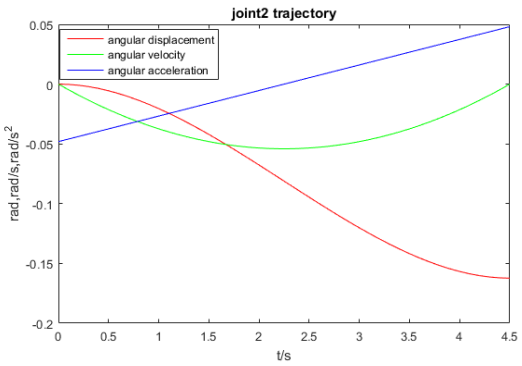

(a) Joint 2 trajectory curve

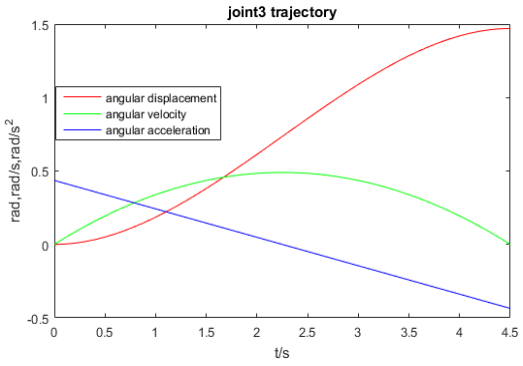

(b) Joint 3 trajectory curve

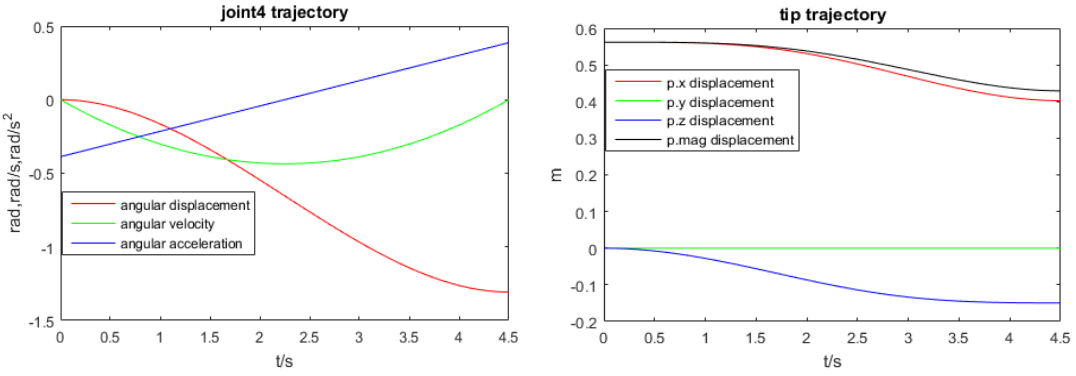

(c) Joint 4 trajectory curve (d) End point trajectory curve

Figure 4. Joint, end point trajectory curve

Fig. 4 visually describes the pickup motion process of the manipulator, where (a), (b) and (c) respectively indicate the angular displacement, angular velocity and angular acceleration trajectory curves of joints 2, 3, and 4, and (d) indicates the end point trajectory curve. The angular acceleration curve changes in an inclined straight line. The absolute value reaches a maximum at the starting and ending moments, and it is in a controllable range avoiding strong shocks. The angular velocity curve is parabolic with no fluctuations. The angular displacement curve is flat at first and then abrupt and finally flat, and smooth transition is achieved. The end point trajectory curve changes smoothly, and the end location point (400mm, 0mm, -150mm) arriving at 4.5s time is consistent with the pickup point, and the grabbing task is completed.

At the same time, the correctness of the inverse kinematics solution of the manipulator is verified by the MATLAB simulation, which lays a good foundation for the solution and movement control of any picking up and placing points in the working area. It is universally applicable for picking up small sports balls.

5. Conclusion

(1) In order to improve the operation flexibility, generality and environmental adaptability of picking up mechanical devices, a 5-DOF pickup manipulator is designed, and the structure composition and functions are introduced.

(2) According to the pickup task requirements of the manipulator, based on the parallel axis theorem and the theorem on moment of resultant force, related theoretical calculation of the required motor driving torque is carried out. Afterwards, based on the working performance characteristics of stepping motor and the parameter settings of different types of stepping motors, 86HS series stepping motors are selected as the drive motors respectively at joints 1, 2 and 3. Besides, the TB6600 stepping motor driver is equipped. Furthermore, the system composition of the stepping motor is analyzed, the design of the stepping motor system is completed, and the closed-loop control of the joint is realized.

(3) Based on the D-H method, the manipulator kinematic model is built. The inverse transformation method is used to calculate the inverse kinematics solution. The kinematics theory analysis is completed, and then MATLAB tool is used to carry out case simulation on the manipulator. The simulation results show that the trajectory curve of each joint is smooth , the motion law is reasonable, and the end point of the manipulator can precisely move to the designated pickup point (400mm, 0mm, -150mm), so as to realize the pickup function of the manipulator.

Acknowledgments

This work was financially supported by Tianjin Natural Science Fund Project (17JCZDJC30400).

References

[1] Andulkar M V, Chiddarwar S S. Incremental approach for trajectory generation of spray painting robot [J]. Industrial Robot, 2015, 42 (3): 228-241.
[2] Gao Feng, Guo Weizhong. Thinking of the Development Strategy of Robots in China [J]. Journal of Mechanical Engineering, 2016, 52 (7): 1-5.
[3] QI Jing, XU Kun, DING Xilun. Vision-Based Hand Gesture Recognition for Human-Robot Interaction: A Review [J]. Robot, 2017, 39 (4): 565-584.
[4] Pacheco L., Oliveira André J.B.de, Ribeiro A.F. Mobile robot for autonomous golf balls picking [C]. Control 2008: proceedings of the Portuguese Conference on Automatic Control Vila Real, Portugal, 2008: 814-818.
[5] Pereira N, F Ribeiro, G Lopes, et al. Autonomous golf ball picking robot design and development [J]. Industrial Robot, 2012, 39 (6): 541-550.
[6] Pereira N, Ribeiro A F, Lopes G, et al. Path planning towards non-compulsory multiple targets using TWIN-RRT [J]. Industrial Robot, 2016, 43 (4): 370-379.
[7] Lv Tengfei, Lu Li, He Binglin, et al. The development of intelligent tennis ball picking machine [J]. Electronics World, 2013, (12): 68-69.
[8] SUN Shijun, PING Xueliang, ZENG Qingyu, et al. Vision-Based Tennis Self-Picking Method Reality [J]. Light Industry Machinery, 2016, 34 (6): 62-65.
[9] Ivan Virgala, František Šimčák, Zdenko Bobovský. Dynamic Analysis of Manipulator Arm for 6-legged Robot [J]. American Journal of Mechanical Engineering, 2013, 1 (7), 365-369.
[10] Patil, Kulkarni, Aswale. Analysis of the inverse kinematics for 5 DOF robot arm using D-H parameters [C]. IEEE International Conference on Real-time Computing and Robotics (RCAR), 2017, 688-693.
[11] Paul R.P., Zhang H. Computational efficient kinematics for manipulators with spherical wrists based on homogeneous transformation representation [J]. International Journal of Robotics Research, 1986, 5 (2): 30-42.
[12] Guo Wanjin, Li Ruifeng, Cao Chuginn. Innovative close-form solution and workspace analysis for a 5-DOF manipulator [J]. Journal of Huazhong University of Science and Technology (Natural Science Edition), 2015, 43 (1): 14-18.
[13] ZHAO Chuan, ZHANG Pengchao, PAN Xiaolei, et al. The robot trajectory interpolation method of research and analysis [J]. Manufacturing Technology & Machine Tool, 2016, (6): 65-69.